

# Catalysts and the structure of SiO<sub>2</sub> sol-gel films

M. A. FARDAD\*

*Optical and Semiconductor Devices Section, Department of Electrical and Electronic Engineering, Imperial college of Science, Technology and Medicine, London SW7 2BT, UK*  
*E-mail: fardad@u.arizona.edu*

In the fabrication of silica films by sol-gel synthesis, the role of various catalysts is systematically examined. The precursor solutions were made by mixing tetraethylorthosilicate (TEOS), ethanol and water in the molar ratio of 1 : 2 : 2. The spin coated films were thermally treated at various temperatures, and characterised using ellipsometry, molecular probe ellipsometry (MPE), infrared spectroscopy (FTIR), scanning electron microscopy (SEM), and optical scattering. By employing different catalysts with the same concentration (0.1 M in water), it was found that dramatic effects on the porosity, optical quality, shrinkage, thickness, structural evolution during thermal treatment, and film stress can be observed. © 2000 Kluwer Academic Publishers

## 1. Introduction

The sol-gel process has been widely shown to be a very flexible route for the fabrication of a large variety of photonic materials in various configurations, such as monoliths, coatings, fibres and films for optical device applications. The formation of oxide particles in a liquid phase, and the polymerisation of the particles make the structure of sol-gel materials inherently porous. The development of the field of semiconductor quantum dots through the sol-gel process in the nineties [1, 2], to enhance the nonlinearity of glass materials, has drawn more attention toward the porosity of sol-gel materials as convenient matrices for the growth of quantum dots. In this laboratory, we are aiming to fabricate thick porous silica-on-silicon waveguides and to fill the porous waveguides with semiconductor microcrystallites (typically CdS, PbS, and solid solutions of these), so as to extend the functionality of glass with possible application in all-optical signal processing. Therefore, a thorough study of the effects of all the parameters involved in the microstructure of fabricated devices is of high significance. This work is the continuation of our earlier work [3–7], and the aim here is systematically to examine the effects of some common catalysts in order to establish a base for future activities.

Silicon alkoxides generally react slowly with water, but the reaction process, hydrolysis and condensation, can be sped up by the use of acid and base catalysts. For example, gelation of TEOS dissolved in ethanol was reduced from 1000 hours to 92 hours when 0.05 concentration of HCl was employed [8]. A number of works have been published on the effects of catalysts on hydrolysis, gelation and properties of bulk gels [9–16]. Aelion *et al.* [9] found that the rate and extent of the hydrolysis reaction of TEOS was most influenced by the strength and concentration of the acid or base used.

They observed that all strong acids behaved similarly, whereas weaker acids required various longer reaction times to achieve the same extent of reaction. Coltrain *et al.* [10] observed that under acidic conditions, the condensation of TEOS ( $R=4$ , where  $R$  is the molar ratio of water to TEOS) was minimised at about pH 2, and maximised at intermediate pH values for various types of acid. The same kind of behaviour had been seen by Iler [11] for condensation of Si(OH)<sub>4</sub>. Pope *et al.* [12] showed that by varying the catalyst in the reaction process of TEOS with water ( $R=4$ ), dramatic effects on gelation time, porosity, density and volume shrinkage on drying may be obtained. They observed that the porosity of the gel heated at 600°C can be increased from 2.8% to 31% by using the same concentration of H<sub>2</sub>SO<sub>4</sub> instead of HCl as the catalyst, while gelation time was increased by 14 hours. The concentration of catalyst (pH) in a silica sol is of considerable importance; its action may vary greatly with only a small change in concentration [11]. The study of porosity by BET and mercury methods in monolithic gels has also shown that the major factor effecting the pore morphology is the type and concentration of catalyst [17]. Schmidt says that the BET surface area from SiO<sub>2</sub> gel can be varied from 0 to 600 m<sup>2</sup>/g simply by varying the concentration of added HCl [15]. Hench *et al.* [18, 19] reported the use of drying control chemical additives (DCCA's) in sol-gel chemistry. They observed that the use of DCCA's like oxalic acid and formamide greatly altered the rates of hydrolysis and condensation reaction and thereby controlled the distribution of pore sizes and solid networks, and hence increased the strength during aging, which in turn increased the drying rate without cracking.

In the fabrication of sol-gel films, acid catalysts (most commonly HCl) are generally used with low amounts

\* Present Address: Optical Sciences Center, University of Arizona, Tucson, AZ 85721 USA.

of water ( $R = 4$ ) [20, 21]. Unlike for bulk gels, no systematic studies of the effects of catalysts on the structure of alkoxide derived films have been reported. However, several works have been published [8, 22–24] which are focused on the effects of pH on the structure of species formed in the solution precursors and hence on the film structure. This work is the first, to our knowledge, to report the influence of catalysts as one of the most important parameters in the sol-gel processing of silica spun films, namely the film porosity.

## 2. Experimental procedure

All the solutions were prepared as follows: 1 mole of tetraethylorthosilicate (TEOS) and 2 moles of ethanol (EtOH) were mixed and stirred at room temperature for 10 min. While stirring, 0.1 M catalysts in water were added dropwise to the solution until a water to TEOS molar ratio of  $R = 2$  was attained. The solutions were then stirred at room temperature for 2 hrs further and aged for 24 hrs before use. All the chemicals were obtained from BDH Merk Ltd, except TEOS which was obtained from the Aldrich Chemical Co.

After ageing of the solutions for 24 hrs, the precipitation of fine particles was visible in the solution catalysed with acetic acid, and it did not adhere onto the microscope slide or silicon wafer, so no film formation was possible by spinning; a similar behaviour was observed for 1 M and 2 M concentration of acetic acid. The solution catalysed with HF gelled, and after dilution did not adhere to the substrates; the same behaviour was observed for 0.01 M and 0.001 M HF. In the case of  $\text{NH}_4\text{OH}$ , after the addition of the catalyst the solution gradually became translucent and then large particles became visible, so that after 24 hrs aging oxide particles were precipitated from the solution and it was unsuitable for use in coating; nevertheless, it was tried but it did not adhere to any substrates. The same behaviour was observed for 0.01 M and 0.001 M  $\text{NH}_4\text{OH}$ . Therefore, the study of  $\text{CH}_3\text{COOH}$ , HF and  $\text{NH}_4\text{OH}$  catalysts were excluded from the rest of this experimental work.

The remaining sols were diluted with ethanol by twice the volume of TEOS before being spin-coated using a S.E.T. TP 60X0 Spin Coater. The sols were dispensed onto p-type silicon wafers through a  $0.1 \mu\text{m}$  filter (PTFE Whatman, supplied by BDH Merk Ltd). Once the substrate was fully covered with the sol, it was spun at 2000 rpm for 30 s. The coated substrate was then cleaved into 10 pieces. Each piece was baked in air at a different temperature, in the range from 100 to  $1000^\circ\text{C}$ , for 30 min. The samples were kept in covered petri dishes in room conditions for a few days before the experiments were continued; this results in the completion of surface hydroxylation, and gives reproducible ellipsometric results when water is used as an adsorbate.

For film stress measurement, TEOS, ethanol, and catalysts in water (mixed with EtOH in equal volume) were mixed in the molar ratios of 1 : 2.3 : 5. Then, the solutions were refluxed from room to  $70^\circ\text{C}$  ( $\sim 3^\circ\text{C}/\text{min}$ ) for 2.5 hrs, and aged for 24 hrs at room temperature. They were then diluted by half the volume before spin coat-

ing. The type of Si wafer, annealing method, annealing temperature, and stress measurement were all as in [3], except the annealing time was 15 s.

The refractive index and thickness of samples were measured using a Rudolph AutoEl III ellipsometer, with an operating wavelength of 632.8 nm, and precision of about  $\pm 0.002$  and  $\pm 3 \text{ \AA}$  in index and thickness, respectively. The porosity and pore size distributions of samples were evaluated employing Molecular Probe Ellipsometry (MPE), in which the dependency of refractive index on partial presence of the absorbed “probe” gas is the basic principle of porosity measurement; a full description of MPE operation is given in [3, 5].

The optical quality of samples was studied as given in Ref. [3]. The surface quality of samples was examined using the optical microscope (Vickers Photoplan 100W) and the scanning electron microscope (JEOL JSM T100).

The molecular structure and composition of films were characterised by Fourier Transform Infrared Spectroscopy (FTIR). IR spectra were recorded in the range of 400 to  $4000 \text{ cm}^{-1}$  at room temperature using FTIR Spectrometer 1760X (Perkin Elmer) with  $5 \text{ cm}^{-1}$  resolution. Transmission and absorption spectra were recorded on films deposited on the p-type silicon wafers (polished on one side) and thermally treated at  $1000^\circ\text{C}$  for 30 min.

## 3. Results

Fig. 1 shows the shrinkage of films as a function of annealing temperature for each acid catalyst. For this and the following figures, the lines between data points are only for the ease of viewing, and the ellipsometric precision results in error ranges that are too small to be indicated in the figures; the precisions in the indicated values of process temperature and relative humidity are approximately  $\pm 1\%$  and  $5^\circ\text{C}$ . Fig. 1 reveals that the shrinkage varies with temperature at different rates for temperatures up to  $1000^\circ\text{C}$ . Compared to the earlier work [3], apparently no oxidation of the Si substrate was evident even at temperatures above  $800^\circ\text{C}$ ;

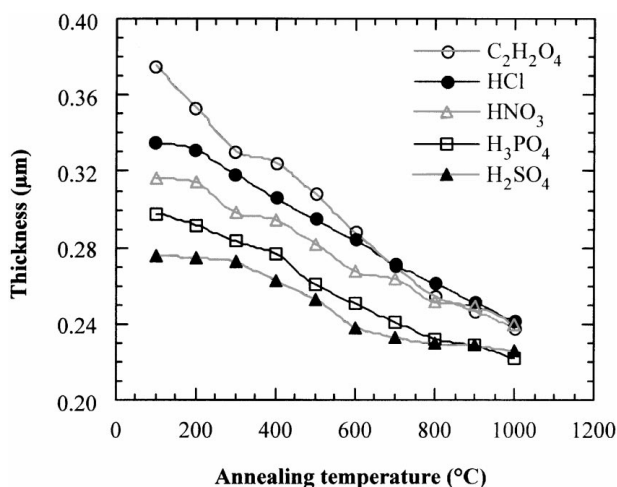


Figure 1 Film thickness vs. annealing temperature (measured in dry  $\text{N}_2$  atmosphere).

this could possibly be due to the higher thickness of these films, which reduce the diffusion of oxygen and thus the rate of thermally grown oxide. Taking viscosity of the sol as one of the main parameters which affect the film thickness, the results presented in the figure for HCl, HNO<sub>3</sub> and H<sub>2</sub>SO<sub>4</sub> films are in agreement with what was observed by Pope *et al.* [12]. They found that the gelation times (1/condensation rate) for these three acids were 92, 100 and 106 hours, respectively. The figure also shows that between the temperature range of 100°C to 1000°C, the C<sub>2</sub>H<sub>2</sub>O<sub>4</sub> films undergo the greatest shrinkage (≈37%), while the H<sub>2</sub>SO<sub>4</sub> films show the most opposition to shrinkage (≈18%). The higher strength of H<sub>2</sub>SO<sub>4</sub> as compared to the other acid catalysts, makes the hydrolysis rate faster; consequently a lower concentration of unreacted OR groups allows less shrinkage during thermal curing. It should be added that the poor surface quality of the H<sub>3</sub>PO<sub>4</sub> films, as will be discussed later, puts some limitation on the precision of ellipsometric measurements in their characterisation.

The evolution of the refractive index and porosity of the films with thermal treatment in a dry N<sub>2</sub> atmosphere is presented in Figs 2 and 3. The films group

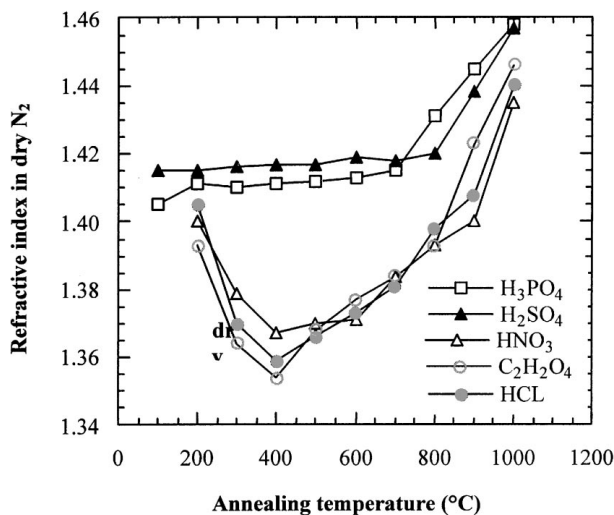


Figure 2 Film refractive index vs. annealing temperature (measured in dry N<sub>2</sub> atmosphere).

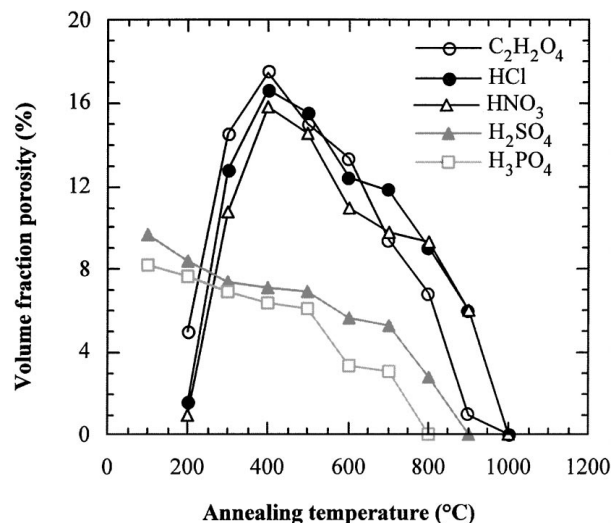


Figure 3 Film porosity vs. annealing temperature.

into two different behaviours with temperature. The first behaviour, which was also observed in the earlier works [3, 4], is that for the HCl, HNO<sub>3</sub> and C<sub>2</sub>H<sub>2</sub>O<sub>4</sub> films. In this case, the indices first decrease up to 400°C, caused by the removal of unreacted organic groups, and the porosities are correspondingly increased; at higher temperature indices then increase because of the start of pore removal and densification. Fig. 3 shows no porosity, at 1000°C, for these three samples, but the refractive indices reached by them at this temperature indicate that there is still some residual porosity left in their structures which are not accessible to the water molecule. The other behaviour belongs to H<sub>3</sub>PO<sub>4</sub> and H<sub>2</sub>SO<sub>4</sub> films. In this case, the porosities decrease monotonically, and equivalently indices increase with temperature and reach that of fused silica (1.46) at 1000°C. Apparently, this behaviour rules out the existence of any unreacted organics in these two films. The slightly higher refractive index of H<sub>3</sub>PO<sub>4</sub> films could be due to the presence of phosphorous, which is employed as a dopant (P<sub>2</sub>O<sub>5</sub>) to increase the refractive index of silica films. Fig. 3 shows that the densification temperature (for the absence of pores) for the H<sub>3</sub>PO<sub>4</sub> film is apparently 800°C, while for the H<sub>2</sub>SO<sub>4</sub> film this temperature is 900°C.

The water vapour absorption isotherm of the films thermal treated at 400°C are plotted in Fig. 4. According to the Brunauer-Emmett-Teller (BET) classification [25], the isotherms are all of type I, indicating that adsorption takes place in microporous systems with pore widths less than 20 Å [26]. As can be seen due to the small size of the pores, all the accessible pores in H<sub>3</sub>PO<sub>4</sub> and H<sub>2</sub>SO<sub>4</sub> films are practically filled at room air humidity, while for other films there are still some pores which can accommodate more water molecules beyond 80% humidity.

The porosity of films was measured using adsorbates of various molecular size by MPE, and the results are shown in Fig. 5a and b. As can be seen the pore size distributions of all samples are broad for all the acid catalysts, and the distribution becomes narrower with increasing annealing temperature. At 400°C, the openings of all the available pores in H<sub>2</sub>SO<sub>4</sub> and H<sub>3</sub>PO<sub>4</sub>

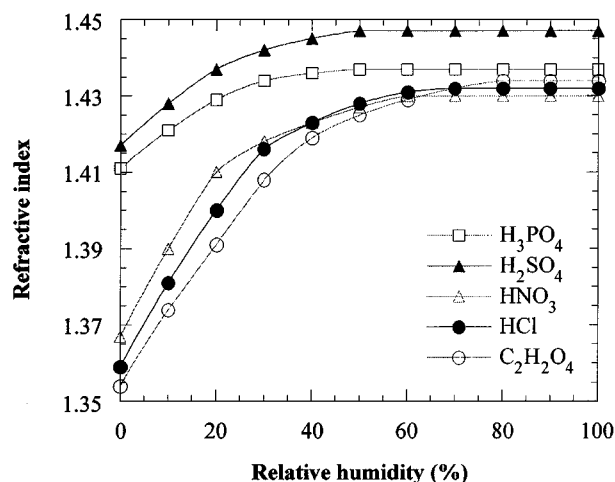


Figure 4 Water vapour isotherms of films annealed at 400°C for 30 minutes.

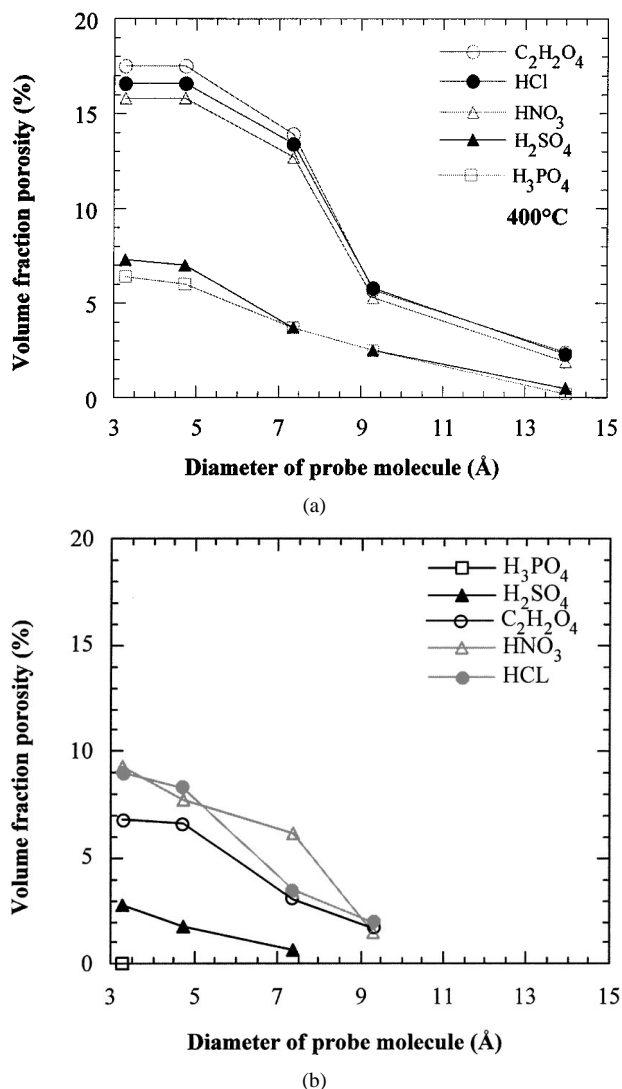


Figure 5 Porosity vs. diameter of probe molecules for: (a) annealing temperature at 400°C and (b) annealing at 800°C.

films are  $\approx 14 \text{ \AA}$ , while at 800°C only a small fraction are greater than 7.5 Å in the H<sub>2</sub>SO<sub>4</sub> films, and no pores are accessible to the water molecule in the H<sub>3</sub>PO<sub>4</sub> films. However, at both temperatures, the other samples keep substantially higher porosity, accessible to the adsor-

bate molecules. The figures also show that at these two temperatures the use of organic-acid DCCA (oxalic acid) does not show any effects on the breadth of pore size distribution as was observed in the bulk gels [18].

After deposition, all the films appeared highly transparent to the naked eye; and optical microscopic investigations revealed striation lines on the surfaces of all films. However, these lines were very faint for H<sub>2</sub>SO<sub>4</sub> samples but more pronounced for C<sub>2</sub>H<sub>2</sub>O<sub>4</sub> samples. After thermal treatment, all the films, except the H<sub>3</sub>PO<sub>4</sub> film, kept their surface qualities and their transparencies were further improved up to temperature 1000°C. However from 200°C, the surface of the H<sub>3</sub>PO<sub>4</sub> film began to peel off in some areas and the peeling became worse at higher temperatures, as shown in Fig. 6. Livage *et al.* [27] observed that the addition of H<sub>3</sub>PO<sub>4</sub> acid to other metal precursors results in rapid precipitation of monophosphates (in this work Si-O-P) rather than formation of polyphosphates. So, the complete destruction of H<sub>3</sub>PO<sub>4</sub> film in some areas must arise from significant loss of materials such as phosphates and H<sub>2</sub>O species.

The optical quality of films was examined by measuring the intensity of scattered light as described in [3]. For each acid catalyst, the ten films baked in the range 100°C to 1000°C were examined and the results are displayed in Fig. 7. The figure shows the mean value of scattered light intensity obtained, and the vertical bars indicate the standard deviation. No systematic variation was observed with respect to the annealing temperatures, except that the C<sub>2</sub>H<sub>2</sub>O<sub>4</sub> films showed a gradual increase in the intensity of scattered light between 800°C to 1000°C. The figure shows that all the films, except the phosphoric acid-catalysed film, have more or less the same optical quality.

Fourier transform infrared (FTIR) absorption spectra in the range of 1400–700 cm<sup>-1</sup> were taken. The films examined were thermal treated at 1000°C for 30 min. The two peak bands characteristic of the Si-O-Si bonds, centred at around 800 cm<sup>-1</sup> and 1080 cm<sup>-1</sup> and due to symmetric and antisymmetric stretching of the oxygen atoms respectively [28], were observed. At 1000°C, Fig. 1 shows that the thickness of H<sub>2</sub>SO<sub>4</sub> and H<sub>3</sub>PO<sub>4</sub> film is  $\approx 0.22 \text{ \mu m}$ , and that of others is  $\approx 0.24 \text{ \mu m}$ .

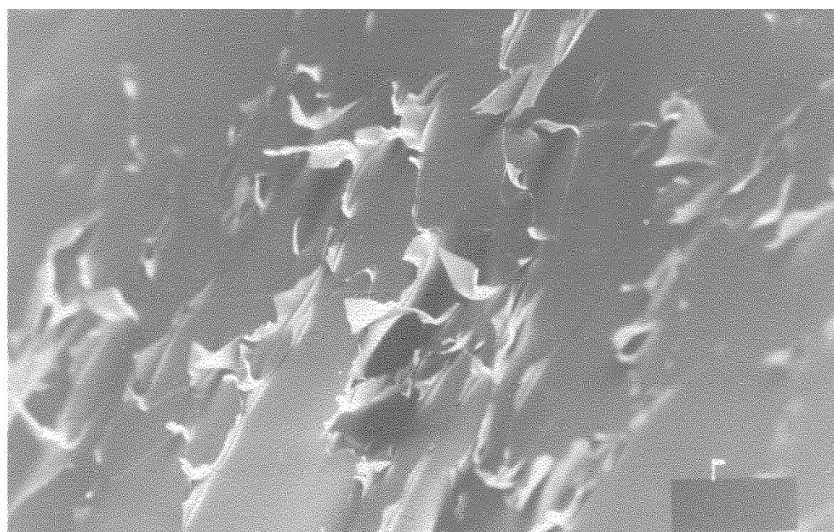


Figure 6 SEM photograph (900 × 600 μm) of H<sub>3</sub>PO<sub>4</sub>-catalysed sol-gel silica film baked at 700°C.

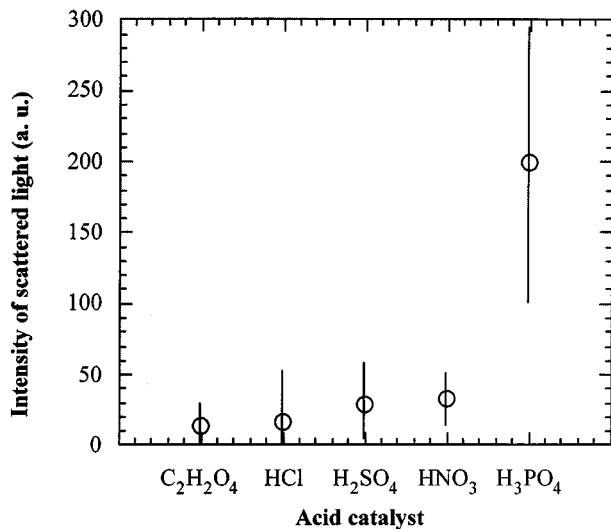


Figure 7 Intensity of scattered light for different acid-catalysed sol-gel silica films. Each data point corresponds to 10 films baked in the range 100°C to 1000°C.

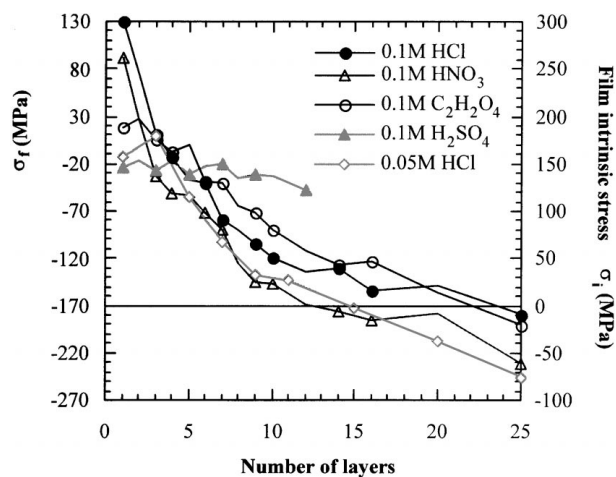


Figure 8 Film stress  $\sigma_f$  vs. number of layers. Each layer was rapid thermal annealed (RTA) at 1000°C for 15 s. The film intrinsic stress  $\sigma_i$  is the extrapolated stress in the film at 1000°C. For the ease of viewing only some data points are shown.

However, the FTIR spectra showed no significant variations in the intensities of peaks due to these thickness differences at these two regions of the spectrum. This is an indication of higher number of siloxane bonds in  $\text{H}_2\text{SO}_4$  and  $\text{H}_3\text{PO}_4$  films compared to the other films. This is quite clear from Fig. 2, which shows that at 1000°C only the refractive indices of  $\text{H}_2\text{SO}_4$  and  $\text{H}_3\text{PO}_4$  films have reached to that of fully dense silica. It also appears that the surfaces of all films are completely dehydroxylated at 1000°C, because the undesirable absorption band of the Si-OH bond at  $\approx 950\text{ cm}^{-1}$  [29, 30] is absent for all films.

The results of the stress measurements are plotted in Fig. 8. The film stress  $\sigma_f$  was determined by measuring the substrate curvature and using Stoney's formula [3]. It was shown in [3] that the film stress has two components  $\sigma_i$  and  $\sigma_{th}$ . The stress at the annealing temperature due to the inherent shrinkage of sol-gel films while constrained onto the substrates is  $\sigma_i$ , and  $\sigma_{th}$  is the stress due to the mismatch between the thermal expansion coefficient of film and substrate as the sample cools down

TABLE I Effects of  $\text{H}_2\text{SO}_4$  concentration (pH) and  $\text{H}_2\text{O}$  on film stress. The concentration of TEOS and EtOH is the same in all the solutions

$\text{H}_2\text{O}$ ( $\text{H}_2\text{SO}_4$ )/ TEOS mol.	Annealing temperature 1000°C	Comment
2 (0.1 M)	Furnace - 2 min	OK at 20 layers ( $-5\ \mu\text{m}$ )
2 (0.1 M)	RTA - 15 s	Failed at 9 layers ( $-2.2\ \mu\text{m}$ )
4 (0.1 M)	RTA - 15 s	Failed at 11 layers ( $-2.4\ \mu\text{m}$ )
5 (0.1 M)	RTA - 15 s	Failed at 13 layers ( $-2.7\ \mu\text{m}$ )
4 (0.05 M)	RTA - 15 s	Failed at 4 layers ( $-0.85\ \mu\text{m}$ )
5 (0.05 M)	RTA - 15 s	Failed at 8 layers ( $-1.7\ \mu\text{m}$ )

from the annealing temperature to room temperature. For the annealing temperature of 1000°C, the  $\sigma_{th}$  component is  $-170\text{ MPa}$  [3]. The film intrinsic stress  $\sigma_i$  can then be determined using  $\sigma_f = \sigma_i - \sigma_{th}$ . For a full description of the stress measurement, the reader is directed to [3]. The figure shows that the stress  $\sigma_f$  in all films is less than zero, i.e. compressive. However, the fabrication of thick multi-layer film ( $\approx 10\ \mu\text{m}$ ) is only possible when film intrinsic stress  $\sigma_i$  systematically decreases as the number of layers increases, and falls well below zero. The crucial parameter is then the annealing temperature, which must be appropriately chosen in order to eliminate the tensile stresses of each layer and to make the film stresses compressive. As can be seen from Fig. 8, only 0.1 M  $\text{HNO}_3$  and 0.05 M  $\text{HCl}$  catalysts are promising for the deposition of thicker films at 1000°C. In the case of 0.1 M  $\text{HCl}$ , the cracks appeared at the edge of film at 25 layers ( $\approx 5.2\ \mu\text{m}$ ); while in the case of 0.05 M  $\text{HCl}$ , although the thickness per layer increased by  $\approx 150\ \text{\AA}$  due to the higher viscosity of sol, the deposition was carried out up to 50 layers ( $\approx 11\ \mu\text{m}$ ) without failure. Tensile stresses in the  $\text{H}_2\text{SO}_4$  catalysed films were always found to be comparatively higher, so that the 0.1 M  $\text{H}_2\text{SO}_4$  film failed at 13 layers ( $2.7\ \mu\text{m}$ ), and the 0.05 M  $\text{H}_2\text{SO}_4$  film failed at 8 layers ( $1.7\ \mu\text{m}$ ). A possible reason is the formation of highly dense small particles with low degree of compliance, which oppose the shrinkage and thus densification. The other possible reason is the fast hydrolysis rate but low condensation rate of species in the solution precursors (Figs 1 and 2); thus the high concentration of hydroxyl groups in the gel films reduces the densification rate [8]. This is clear in Table I; the table shows that thicker films can be built up from the same sol when the conventional furnace is used for annealing each layer for 2 min rather than RTA for 15 s.

#### 4. Discussion

Hydrolysis and condensation of silicon alkoxides can be dramatically influenced by employing catalysts. Different catalysts result in gels with different properties and microstructures, which, according to Pope *et al.* [12], can be related to the differences in the catalytic

mechanism. In the presence of ethanol and below stoichiometric water ( $R = 2$ ),  $H_2SO_4$  and  $H_3PO_4$  speed up the hydrolysis rate of the ethoxy groups (-OR) of TEOS compared to the condensation rate. Thus, the low viscosity of sols yields thinner spun films (Fig. 1), but more porous as-deposited gel films (Fig. 3). This is due to the formation of peculiar particles in the solutions with high concentration of hydroxyl groups (-OH) which condense to some extent during film deposition and oppose the compactness of film structures, thus increasing the porosity of the as-deposited films. This condensation of species in turn increases the strength of gel films and consequently films shrink less during thermal treatment (Fig. 1). The use of these two acid catalysts indicates the absence of unreacted ethoxy groups, and therefore cancels out their contribution to the tensile stress during shrinkage [29]. In the case of  $H_3PO_4$ , it should be added that phosphorous is trivalent or pentavalent rather than tetravalent, therefore it is expected to be a network modifier and to reduce the densification temperature, which has been proven in the fabrication of thick multi-layer sol-gel phosphosilicate glass films [31]. Although phosphoric acid-catalysed films showed the same behaviour as sulphuric acid-catalysed films, the very poor quality of these films (Fig. 6) makes them undesirable for device applications.

Compared with  $H_2SO_4$  and  $H_3PO_4$ , catalysts such as HCl,  $HNO_3$  and  $C_2H_2O_4$  in the presence of ethanol and 2 moles of water retard the hydrolysis compared to the condensation rate. Thus, the higher viscosity of the solution precursors results in thicker spun films (Fig. 1). However, due to the lower concentration of OH groups the structure experiences less condensation and it collapses to some extent during film formation, and consequently results in less porous as-deposited films (Fig. 3). Due to this high presence of OR groups, the films shrink to a greater extent during thermal treatment (Fig. 1) and as a result the porosity of such films increases dramatically (Fig. 3). Consequently, the tensile stress due to the high shrinkage is expected to be higher in these films. In this group of catalysts, oxalic acid, known as an acidic DCCA, yields film with even higher shrinkage, porosity and faster densification rate during heat treatment. The higher porosity could be due to its lower strength compared to HCl and  $HNO_3$ , while the faster densification rate could be due to the more uniform structure of gel film as a result of the DCCA effect [18], although MPE results (Fig. 5) show no evidence on narrower pore size distribution of the oxalic acid films.

In the study of HCl,  $HNO_3$  and  $H_2SO_4$ , the viscosity of solutions (deduced from the film thicknesses) obtained from the use of these acid catalysts, as well as the porosity of as-deposited films and the shrinkage during thermal treatment, are all in agreement with what was observed by other workers [12, 28] in the production of bulk silica gels. Catalysts like HCl,  $HNO_3$ ,  $C_2H_2O_4$ , and  $H_2SO_4$  yield films which contain nanopores whose openings to the external surface have widths which mostly lie in the range  $\approx 10 \text{ \AA}$ , with a broad pore size distribution (Fig. 5). These films are of high optical quality and within the standard requirements of integrated

optical devices (Fig. 7). However, the low porosity of  $H_2SO_4$  and  $H_3PO_4$  catalysed films and the high porosity of HCl,  $HNO_3$  and  $C_2H_2O_4$  catalysed films (Figs 3 and 5) make the former catalysts less attractive and the latter ones more attractive for the field of quantum dot film waveguide fabrication. Finally, the sols prepared from various concentration of  $CH_3COOH$ , HF and  $NH_4OH$  showed the same behaviour on the substrates (microscope slides and p-type (100) silicon wafers), i.e. they did not adhere onto the substrates, and were unsuitable for spin-coating. In the case of  $CH_3COOH$  and  $NH_4OH$  large particles precipitated, so that the formation of a stable suspension of oxide particles suitable for film drawing was not possible.

Among other parameters, stress in the sol-gel spin-coated films fabricated in this work was found to depend on the concentration of water, type and concentration (pH) of catalyst employed. The employment of different catalysts in this study shows that the stress does not merely depend on the magnitude of shrinkage during thermal treatment. For example, the use of sulphuric acid resulted in the formation of highly dense small particles with the lowest viscosity and shrinkage (Fig. 1) while with the greatest stress (Fig. 8). Therefore, the structure of species formed in the solution precursor and the concentration of hydroxyl groups both greatly affect the densification rate, thus film stress. The role of OH groups on the film stress was further proved by using 0.05 M HCl instead of 0.1 M HCl in the presence of constant water; although the thickness of each layer was increased by around  $150 \text{ \AA}$  (high condensation rate and viscosity, and therefore low presence of the hydroxyl groups), the film stress was reduced (Fig. 8). Since higher condensation rate in a solution is an indication of larger species, it should be concluded that the use of HCl results in the formation of species with high degree of compliance, which densify quickly.

## 5. Conclusion

In the fabrication of silica sol-gel films based upon the hydrolysis and condensation of TEOS with 2 moles of water, and in the presence of 2 moles of ethanol, the influence of various catalysts on the film structures was investigated. The investigation shows that the film thickness, shrinkage, porosity, and optical quality depend on the type of catalyst used in the preparation of the solution precursor. Amongst the catalysts studied, three different behaviours were observed. The first behaviour belongs to  $CH_3COOH$ , HF and  $NH_4OH$ . Different concentrations of  $CH_3COOH$  and  $NH_4OH$  resulted in the precipitation of particles in the solutions, which did not adhere to the glass slide and p-type Si substrates; the same property was shown by HF, though the solution was homogeneous. Based on the recipe followed in this study, the usefulness of these three catalysts used alone, was therefore excluded for the spin coating process of silica films. The second behaviour comprises HCl,  $HNO_3$  and  $C_2H_2O_4$ . These catalysts yield films with nearly the same optical qualities and microstructures which undergo similar evolution during thermal treatment. The third behaviour belongs to  $H_2SO_4$  and

H<sub>3</sub>PO<sub>4</sub>. Compared with the second behaviour, these two catalysts give more porous as-deposited films which are thinner and shrink less with significantly less porosity during heat treatment. The very poor optical quality of H<sub>3</sub>PO<sub>4</sub> catalysed films makes them unsuitable for device applications. The higher overall porosity of the second group of catalysts makes them more attractive for the fabrication of semiconductor doped waveguides leading to all-optical switching devices. Finally, the stress in the sol-gel films is sensitive to the type and concentration of catalyst used; by choosing a particular catalyst and adjusting its concentration (pH), the stress can be greatly reduced.

### Acknowledgement

The author would like to thank Dr. Eric Yeatman and Professor Mino Green for their useful comments and suggestions. The financial support of the Science and Engineering Research Council (SERC) and of the European Commission under the Esprit programme (project 6993: NODES), are also gratefully acknowledged.

### References

1. M. NOGAMI and K. NAGASAKA, *J. Non-Cryst. Solids* **122** (1990) 101.
2. W. E. TORRUELLAS, L. A. WELLER-BROPHY, R. ZANONI and G. I. STEGEMAN, *Appl. Phys. Lett.* **58**(11)(1991) 1128.
3. M. A. FARDAD, E. M. YEATMAN, E. J. C. DAWNAY, MINO GREEN and F. HOROWITZ, *J. Non-Cryst. Solids* **183** (1995) 260.
4. M. A. FARDAD, E. M. YEATMAN and E. J. C. DAWNAY, in Proc. SPIE, Sol-Gel Optics III, edited by J. D. Mackenzie (1994), Vol. 2288, p. 77.
5. E. M. YEATMAN, MINO GREEN, E. J. C. DAWNAY, M. A. FARDAD and F. HOROWITZ, *J. Sol-Gel Sci. Technol.* **2** (1994) 711.
6. E. J. C. DAWNAY, M. A. FARDAD, MINO GREEN, F. HOROWITZ, E. M. YEATMAN, R. M. ALMEIDA, H. C. VASCONCELOS, M. GUGLIELMI and A. MARTUCCI, in "Advanced Materials in Optics, Electro-Optics and Communication Technologies," edited by P. Vincenzini and G. C. Righini (Techna Srl, 1995).
7. F. HOROWITZ, E. M. YEATMAN, E. J. C. DAWNAY and M. A. FARDAD, *J. Phys. III France* **3** (1993) 2059.

8. C. J. BRINKER and G. W. SCHERER, "Sol-Gel Science, The Physics and Chemistry of Sol-Gel Processing" (Academic Press Inc., 1990).
9. R. AELION, A. LOEBEL and F. EIRICH, *J. Am. Chem. Soc.* **72** (1950) 5705.
10. B. K. COLTRAIN, S. M. MELPOLDER and J. M. SALVA, in "Ultrastructure Processing of Advanced Materials," edited by D. R. Uhlaman and D. R. Ulrich (John Wiley & Sons Inc., 1992) p. 69.
11. R. K. ILLER, "The Chemistry of Silica" (Wiley, New York, 1973).
12. E. J. A. POPE and J. D. MACKENZIE, *J. Non-Cryst. Solids* **87** (1986) 185.
13. T. W. ZERDA, I. ARTAKI and J. JONAS, *ibid.* **81** (1986) 365.
14. M. NOGHAMI and Y. MORIYA, *ibid.* **37** (1980) 191.
15. H. SCHMIDT, *ibid.* **100** (1988) 51.
16. J. Y. YING and J. B. BENZIGER, *J. Am. Ceram. Soc.* **76**(10) (1993) 2571.
17. A. J. MARTIN, PhD thesis, Imperial College, U.K., 1991.
18. L. L. HENCH, in "Science of Ceramic Chemical Processing," edited by L. L. Hench and D.R. Ulrich (Wiley-Interscience, 1986) p. 52.
19. G. ORCEL and L. L. HENCH, *Mat. Res. Soc. Symp. Proc.* **32** (1984) 79.
20. J. D. MACKENZIE, in Proc. SPIE, Sol-Gel Optics III (1994) Vol. 2288.
21. S. SAKKA, *J. Sol-Gel Science and Technology* **2** (1994) 451.
22. C. J. BRINKER, A. J. HURD, P. R. SCHUNK, G. C. FRYE and C. S. ASHLEY, *J. Non-Cryst. Solids* **147/148** (1992) 424.
23. M. C. MATOS, A. R. CARVALHO and R. M. ALMEIDA, in Proc. SPIE (1992), Vol. 1758, p. 77.
24. C. J. BRINKER, G. C. FRYE, A. J. HURD, K. J. WARD and C. S. ASHLEY, in "Ultrastructure Processing of Advanced Materials," edited by D. R. Uhlmann and D. R. Ulrich (John Wiley & Sons Inc., 1992) p. 211.
25. S. BRUNAUER, P. H. EMMETT and E. TELLER, *J. Am. Chem. Soc.* **60** (1938) 309.
26. S. G. GREGG and K. S. W. SING, "Absorption, Surface Area and Porosity, 2nd ed." (Academic Press, New York, 1982).
27. J. LIVAGE, P. BARBOUX, M. T. WANDENBORRE, C. SCHMUTZ and F. TAULELLE, *J. Non-Cryst. Solids* **167** (1994) 16.
28. J. D. MACKENZIE, in "Science of Ceramic Chemical Processing," edited by L. L. Hench and D. R. Ulrich (Wiley-Interscience, 1986) p. 113.
29. T. M. PARRILL, *J. Mater. Res.* **9** (1994) 723.
30. R. M. ALMEIDA and C. G. PANTANO, *J. Appl. Phys.* **68** (1990) 4225.
31. R. R. A. SYMS, *J. Non-Cryst. Solids* **167** (1994) 16.

Received 7 May 1996

and accepted 10 February 1998